



Article

Automobile Exhaust Removal Performance of Pervious Concrete with Nano TiO₂ under Photocatalysis

Guobao Luo ^{1,2} , Hanbing Liu ³, Wenjun Li ^{3,*} and Xiang Lyu ³

¹ State Key Laboratory of Mechanical Behavior and System Safety of Traffic Engineering Structures, Shijiazhuang Tiedao University, Shijiazhuang 050043, China; luogb@stdu.edu.cn

² Key Laboratory of Roads and Railway Engineering Safety Control (Shijiazhuang Tiedao University), Ministry of Education, Shijiazhuang 050043, China

³ College of Transportation, Jilin University, Changchun 130025, China; lhb@jlu.edu.cn (H.L.); lvxiang18@mails.jlu.edu.cn (X.L.)

* Correspondence: wenjun18@mails.jlu.edu.cn; Tel.: +86-159-4307-6974

Received: 29 September 2020; Accepted: 20 October 2020; Published: 21 October 2020



Abstract: The urban environment is facing serious problems caused by automobile exhaust pollution, which has led to a great impact on human health and climate, and aroused widespread concern of the government and the public. Nano titanium dioxide (TiO₂), as a photocatalyst, can be activated by ultraviolet irradiation and then form a strong REDOX potential on the surface of the nano TiO₂ particles. The REDOX potential can degrade the automobile exhaust, such as nitrogen oxides (NO_x) and hydrocarbons (HC). In this paper, a photocatalytic environmentally friendly pervious concrete (PEFPC) was manufactured by spraying nano TiO₂ on the surface of it and the photocatalytic performance of PEFPC was researched. The nano TiO₂ particle size, TiO₂ dosage, TiO₂ spraying amount, and dispersant dosage were selected as factors to investigate the efficiency of photocatalytic degradation of automobile exhaust by PEFPC. Moreover, the environmental scanning electron microscope (ESEM) was used to evaluate the distribution of nano TiO₂ on the surface of the pervious concrete, the distribution area of nano TiO₂ was obtained through Image-Pro Plus, and the area ratio of nano TiO₂ to the surface of the pervious concrete was calculated. The results showed that the recommended nano TiO₂ particle size is 25 nm. The optimum TiO₂ dosage was 10% and the optimum dispersant dosage was 5.0%. The photocatalytic performance of PEFPC was best when the TiO₂ spraying amount was 333.3 g/m². The change in the photocatalytic ratio of HC and NO_x is consistent with the distribution area of nano TiO₂ on the surface of the pervious concrete. In addition, the photocatalytic performance of PEFPC under two light sources (ultraviolet light and sunlight) was compared. The results indicated that both light sources were able to stimulate the photocatalytic performance of PEFPC. The research provided a reference for the evaluation of automobile exhaust removal performance of PEFPC.

Keywords: photocatalysis; nano TiO₂; ESEM; nitrogen oxides; hydrocarbons; pervious concrete

1. Introduction

In recent decades, global urbanization and development of the automotive industry have caused many environmental problems while promoting rapid social development [1,2]. Urban air pollution, as the most serious one, has had a great impact on urban environment and human health [3]. Automobile exhaust caused by the increasing number of motor vehicles in the city is the main source of urban air pollution. The main components of automobile exhaust are nitrogen oxides (NO_x) and hydrocarbons (HC). Sustainability development, especially environmental sustainability development, has become a

key issue of social development and aroused widespread concern of the government and the public [4]. Automobile exhaust leads to air pollution throughout the world. There are many emission reduction methods, such as the encouragement of carpooling and public transportation, but automobile exhaust pollution is still a serious problem all over the world [5].

Nano titanium dioxide (TiO_2), characterized by low toxicity, strong optical absorption, and redox ability, and is promising in photocatalytic degradation of automobile exhaust [6,7]. Moreover, nano TiO_2 has a wide band gap of about 3.2 eV and has significant performance in the ultraviolet light region [8], and automobile exhaust photocatalytic products are harmless to the urban environment [9–11]. In recent years, the rapid development of TiO_2 photocatalytic technology has prompted the application of photocatalytic pavement materials to improve urban air quality [12,13]. Nano TiO_2 is the most extensively used photocatalyst due to its low cost and high chemical stability [14,15]. Pervious concrete is considered to be an environmentally friendly pavement material, which has many environmental benefits, such as improving water quality and reducing soil pollution. The use of pervious concrete meets the requirements of sustainable social development [16]. The incorporation of nano TiO_2 into pervious concrete pavement materials imparts photocatalytic performance to pervious concrete [17–19]; automobile exhaust nearby pervious concrete pavement can be converted to water and salt under ultraviolet light irradiation and subsequently the salt will be washed away by the rain [20,21].

Nano TiO_2 exists in three different crystalline forms: anatase, rutile, and brookite [22]. Anatase TiO_2 has an indirect bandgap while rutile has a direct bandgap. The ability of indirect bandgap to inhibit the recombination of the electron and hole is better than that of direct bandgap, which results in anatase TiO_2 , which is better than rutile TiO_2 in photocatalytic activity [23]. It is difficult to produce brookite TiO_2 in the laboratory due to its intermediate phase in the anatase to brookite to rutile [24]. Under ultraviolet irradiation, electrons in the valence band are activated and transferred into the conduction band, leaving relatively stable holes on the surface of the valence band, thus forming electron–hole pairs. The electron and hole are captured by imperfection and dangling bond of nano TiO_2 and diffuse to the surface of nano TiO_2 , forming a strong REDOX potential and degrading automobile exhaust into harmless substances. For various reasons, anatase TiO_2 is the preferred photocatalyst due to its strong photocatalytic activity, simple preparation and the absence of toxicity [18,23].

In recent years, many experiments have been performed under different experimental conditions in order to evaluate the photocatalytic performance of nano TiO_2 and promote the application of photocatalytic pavement materials. Some scholars have studied the effects of substrate materials on the photocatalytic performance of nano TiO_2 . Xu et al. [25] studied the effect of recycled aggregate on the photocatalytic performance of nano TiO_2 concrete. The results showed that the recycled aggregate coated with nano TiO_2 significantly improved the photocatalytic performance of nano TiO_2 concrete. Chen et al. [13] used recycled glass to replace sand in preparing the concrete; the effects of glass color, aggregate size, and curing age on the photocatalytic performance of nano TiO_2 concrete were investigated. The significant improvement of photocatalytic performance was obtained due to the use of recycled glass in the concrete. Guo et al. [12] evaluated the effects of white cement and ground granulated blast furnace slag on the photocatalytic performance of nano TiO_2 concrete. The results showed that the use of white cement and ground granulated blast furnace slag had a positive effect on photocatalytic performance of nano TiO_2 concrete. Some scholars have studied the effect of environmental factors on photocatalytic performance of nano TiO_2 . Guo et al. [26] compared the effects of different NO flow rates, initial NO concentrations, ultraviolet light intensities, and relative humidity conditions on the photocatalytic performance of nano TiO_2 concrete. Ballari et al. [18] studied the effects of initial NO_x concentration, reactor height, and flow rate on the photocatalytic performance of nano TiO_2 concrete and proposed the corresponding kinetic model. However, research about the photocatalytic degradation of HC is not enough, and even fewer studies were reported on the effect of dispersion of TiO_2 on photocatalytic performance.

In this study, in allusion to the problem of excessive automobile exhaust, the photocatalytic performance of PEFPC was evaluated. The TiO_2 particle size, TiO_2 dosage, TiO_2 spraying amount and

dispersant dosage were selected as effect factors and the experiment of photocatalytic performance of PEFPC was conducted, and the distribution of nano TiO₂ on the surface of PEFPC was evaluated by the environmental scanning electron microscope (ESEM). Moreover, the photocatalytic performance of PEFPC under two light sources (ultraviolet light and sunlight) was compared and the application of PEFPC was evaluated. The research outline of the study is shown in Figure 1.

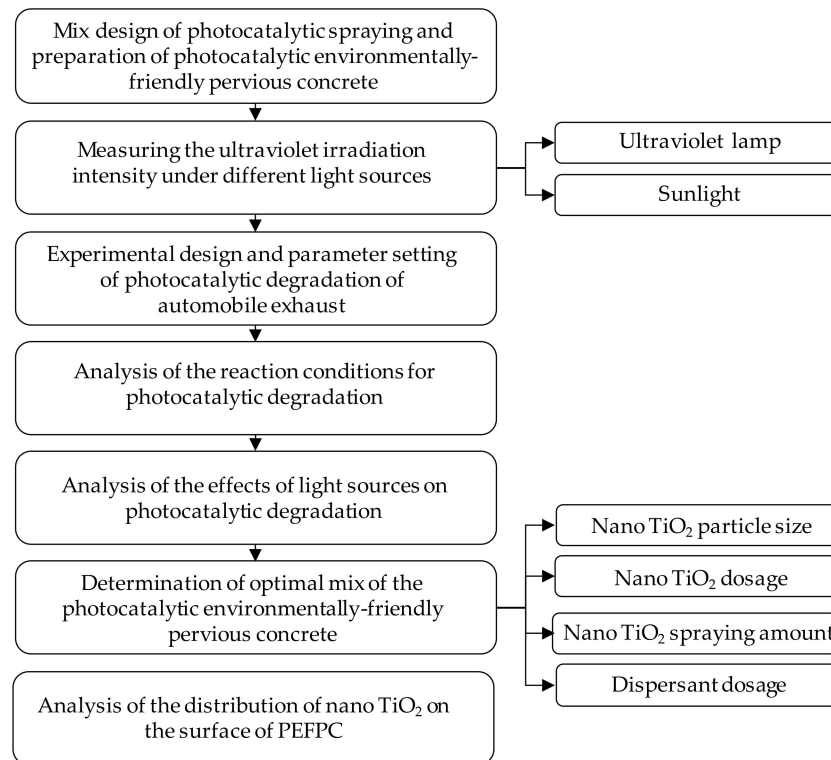


Figure 1. Research outline.

2. Photocatalytic Degradation Mechanism

Ultraviolet light irradiates the surface of nano TiO₂, and the photons in the ultraviolet light are captured by nano TiO₂. The photons with an energy equal to or greater than the band gap can activate the electrons in the valence band of nano TiO₂. The activated electrons jump into the conduction band, thus resulting in the generation of holes in the valence band. The electron–hole pairs may rapidly recombine and release energy, or are captured by the surface of nano TiO₂ to form a REDOX potential. The electrons and holes have strong reducibility and strong oxidability, respectively. The holes react with water to form strong oxidizing hydroxyl radicals. The electrons react with oxygen to form superoxide anions, which have strong REDOX properties. NO_x is oxidized to nitrate by hydroxyl radicals and superoxide anions. HC is oxidized and reduced to water and carbon dioxide by hydroxyl radicals and superoxide anions [27,28]. It is the basis condition for photocatalytic reaction that nano TiO₂ molecules capture a sufficient number and energy of photons. The number of captured photons is related to the contact area of nano TiO₂ molecules and ultraviolet light. The contact area was affected by TiO₂ particle size, TiO₂ dosage, TiO₂ spraying amount, and dispersant dosage. The energy of photons is related to the intensity of ultraviolet light. In this study, the effects of contact area of nano TiO₂ molecules and ultraviolet light and the intensity of ultraviolet light on the photocatalytic degradation HC and NO_x were investigated.

3. Materials and Methods

3.1. Materials

In all experiments, Type P.O Portland cement (Changchun, China) with strength grade of 42.5 MPa was selected as the cementitious materials. The chemical composition of cement is shown Table 1. The natural aggregate with particle of 4.75–9.5 mm was used as coarse aggregate to prepare pervious concrete. The water reducer used was liquid polycarboxylic acid series superplasticizer with effective content of 22% and water-reducing ratio of 25%. An anatase nano TiO₂ obtained from Chengdu Oenris Chemical Reagent Co., Ltd. (Chengdu, China) was used as photocatalyst. The particle size of the TiO₂ is 10 nm (5–15 nm), 25 nm (20–30 nm), and 50 nm, and its purity is 99%. The sodium hexametaphosphate ((NaPO₃)₆) obtained from Chengdu Oenris Chemical Reagent Co., Ltd. (Chengdu, China) was used as dispersant. The sodium hexametaphosphate is analytically reagent and its purity is 65–70%.

Table 1. The chemical composition of cement.

Material	Chemical Composition (%)					
	SiO ₂	Al ₂ O ₃	Fe ₂ O ₃	CaO	MgO	SO ₃
Cement	22.60	5.60	4.30	62.70	1.70	2.50

The VDW (Van der Waals' force) and coulomb force exist in between nano TiO₂ particles, which leads to the particles absorbing and aggregating with each other, thus losing the dispersion stability of the particles in the suspension. The aggregated nano TiO₂ particles are shown in Figure 2a. Sodium hexametaphosphate can form a stable complex with nano TiO₂ molecules. The complex increases the Zeta potential on the surface of the nano TiO₂ particles and leads to the increase in the repulsive force between nano TiO₂ particles, thus improving the dispersion stability of nano TiO₂ particles in the suspension [29]; the nano TiO₂ particles after adding dispersant are shown in Figure 2b.

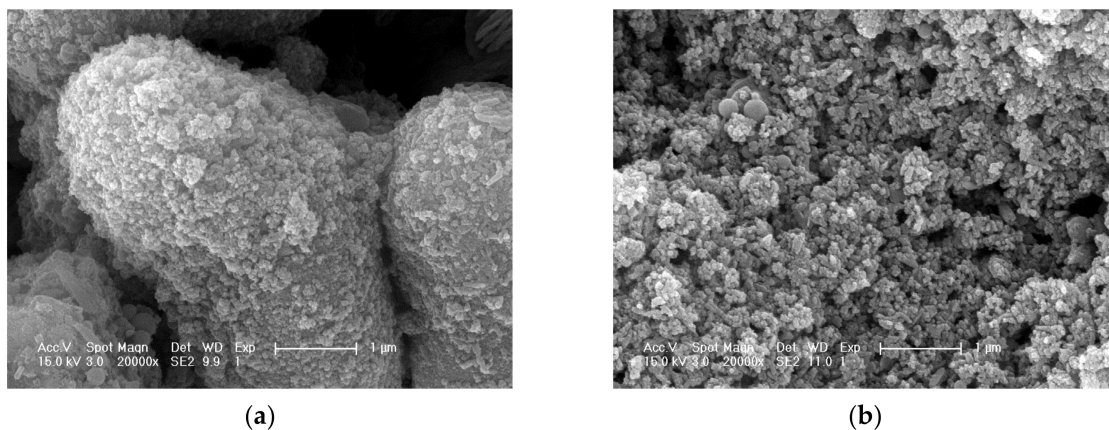


Figure 2. Nano titanium dioxide (TiO₂): (a) before adding dispersant; (b) after adding dispersant.

3.2. Preparation of the Photocatalytic Environmentally Friendly Pervious Concrete

The volumetric method was used for the mixture design of pervious concrete according to the Chinese national standard CJJ/T135-2009 [30]. Based on the previous research conducted by our group [31,32], pervious concrete with optimal mixing ratio was used as substrate materials in this paper, the permeability and effective porosity reached above 3.90 mm/s and 14%, respectively, and the compressive strength was 24 MPa. Moreover, pervious concrete specimens were made using the cement paste encapsulating aggregate method and rodding method. The water–binder ratio and porosity were 0.30 and 15%, respectively. The amount of water reducer was 0.5% of the mass of

cement. The specimen size was $300 \times 300 \times 50$ mm. All the specimens were demolded after 24 h and placed in standard-cured room with a relative humidity of 95% and a temperature of 20 ± 2 °C for 28 days. Nano TiO₂ and sodium hexametaphosphate were dispersed into water to prepare TiO₂ coating, and then the TiO₂ coating was sprayed on the surface of pervious concrete and tested after natural air drying for 24 h. The dispersant dosage is the mass percentage of nano TiO₂. The mixing ratio of photocatalytic coating is shown in Table 2.

Table 2. Mixing ratio of photocatalytic coating.

Mix ID	TiO ₂ Particle Size (nm)	TiO ₂ Dosage (%)	TiO ₂ (g)	TiO ₂ Spraying Amount ¹ (g/m ²)	TiO ₂ Spraying Amount (g)	Dispersant Dosage (%)	Dispersant (g)
PZ1	10	10	3.0	333.3	30	5.0	0.150
PZ2	25	10	3.0	333.3	30	5.0	0.150
PZ3	50	10	3.0	333.3	30	5.0	0.150
D1	25	3	0.9	333.3	30	5.0	0.045
D2	25	5	1.5	333.3	30	5.0	0.075
D3	25	10	3.0	333.3	30	5.0	0.150
D4	25	15	4.5	333.3	30	5.0	0.225
D5	25	20	6.0	333.3	30	5.0	0.300
SD1	25	10	1.0	111.1	10	5.0	0.050
SD2	25	10	2.0	222.2	20	5.0	0.100
SD3	25	10	3.0	333.3	30	5.0	0.150
SD4	25	10	4.0	444.4	40	5.0	0.200
SD5	25	10	5.0	555.5	50	5.0	0.250
DD1	25	10	3.0	333.3	30	0	0
DD2	25	10	3.0	333.3	30	2.5	0.075
DD3	25	10	3.0	333.3	30	5.0	0.150
DD4	25	10	3.0	333.3	30	7.5	0.225
DD5	25	10	3.0	333.3	30	10.0	0.300
LR1	25	10	3.0	333.3	30	5.0	0.150
LR2	25	10	3.0	333.3	30	5.0	0.150
LR3	25	10	3.0	333.3	30	5.0	0.150
LR4	25	10	3.0	333.3	30	5.0	0.150
Null				333.3	30		

¹ the surface of area of pervious concrete is 0.09 m², PZ refers to the TiO₂ particle size, D refers to the TiO₂ dosage, SD refers to the TiO₂ spraying amount, DD refers to the dispersant dosage, LR refers to the light source. Null refers to control group.

3.3. Determination of Light Intensity

Nano TiO₂ can be motivated to produce electrons and holes under ultraviolet irradiation. An ultraviolet lamp was used as the experimental light source and the ultraviolet wavelength is 285–297 nm. 17 measurement points on the surface of the specimen were chosen, which are shown in Figure 3a. The ultraviolet lamp and specimen were placed in the middle of the reactor. The ultraviolet irradiance meter was used to measure the ultraviolet irradiation intensity of the measured points at different ultraviolet lamp heights. Just as shown in Figure 3b,c, the ultraviolet lamp was placed directly above the specimen and the distance between the ultraviolet lamp and the center of the specimen was 135 mm, 180 mm, 225 mm, and 270 mm, respectively. The average ultraviolet irradiation intensity at different ultraviolet lamp heights was calculated and the results are shown in Table 3. The ultraviolet irradiation intensity on the hour of the summer solstice was measured, which is shown in Figure 3d. The average ultraviolet irradiation intensity of the day was calculated, and the result is shown in Table 3.

Table 3. Ultraviolet irradiation intensity of ultraviolet lamp and sunlight.

Light Source	UV Height 135 mm	UV Height 180 mm	UV Height 225 mm	UV Height 270 mm	Sunlight
Ultraviolet irradiation intensity ($\mu\text{W}/\text{cm}^2$)	105.1	48.4	31.8	19.1	104.9

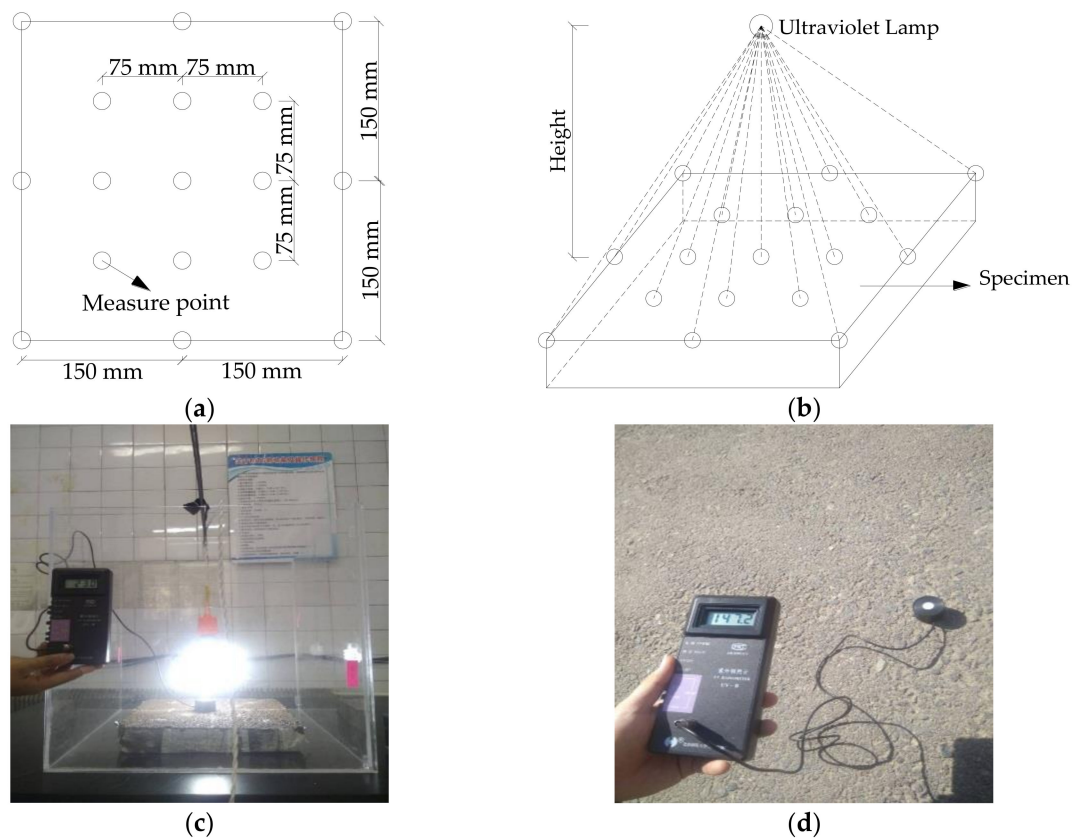


Figure 3. Ultraviolet irradiation intensity experiment of ultraviolet lamp and sunlight: (a) measuring point diagram; (b) test diagram; (c) ultraviolet intensity test; (d) sunlight intensity test.

3.4. Photocatalytic Degradation Experiment

The experimental device consisted of three parts: automobile exhaust analysis device, reactor, and automobile exhaust source, as shown in Figure 4a–c. The reactor was completely sealed and had a good air tightness. The size of reactor is $450 \times 450 \times 500$ mm. MQW-50A tail gas analyzer obtained from Zhejiang University Mingquan Electronic Technology Co., Ltd. (Hangzhou, China) was used to analyze the automobile exhaust components. The measurement range of NO_x and HC was 0–5000 ppm and 0–10,000 ppm respectively and the relative measurement error was 4% and 3%, respectively. Both NO_x and HC had a resolution of 1 ppm. The experimental procedures are as follows: (1) put the specimen into the bottom middle position of the reactor and adjust the height of the ultraviolet lamp as shown in Figure 4b; (2) connect the automobile exhaust source to the reactor with a rubber hose as shown in Figure 4c; (3) add automobile exhaust into the reactor and turn on the automobile exhaust analysis device for real-time monitoring until the initial concentrations of NO_x and HC are reached; (4) cover the reactor with a shading cloth to prevent interference with natural light and then turn on the ultraviolet lamp for the test as shown in Figure 4d. All experiments were performed at ambient temperature and one atmosphere. The concentrations of NO_x and HC in the actual traffic jam section are about 15 ppm and 35 ppm, respectively. Therefore, the initial concentrations of NO_x and HC in this experiment were set as 80 ppm and 160 ppm, respectively. The reaction time was 60 min, and the NO_x and HC concentrations in the reactor were tested every 10 min. The photocatalytic degradation ratios of NO_x and HC on the surface of PEFPC are calculated as Equation (1). The photocatalytic degradation rates of NO_x and HC on the surface of PEFPC are calculated as Equation (2).

$$D = \frac{G_{\text{intial}} - G_{\text{final}}}{G_{\text{intial}}} \times 100\% \quad (1)$$

$$F = \frac{G_{initialN} - G_{finalN}}{T} \quad (2)$$

where D is the photocatalytic degradation ratio of NO_x and HC (%); $G_{initial}$ is the initial concentration of NO_x and HC (ppm); G_{final} is the final concentration of NO_x and HC (ppm); F is the photocatalytic degradation rate of NO_x and HC (ppm/min); $G_{initialN}$ is the initial concentration of NO_x and HC in the N th ten minutes (ppm); G_{finalN} is the final concentration of NO_x and HC in the N th ten min (ppm); T is the reaction time and $T = 10$ min.

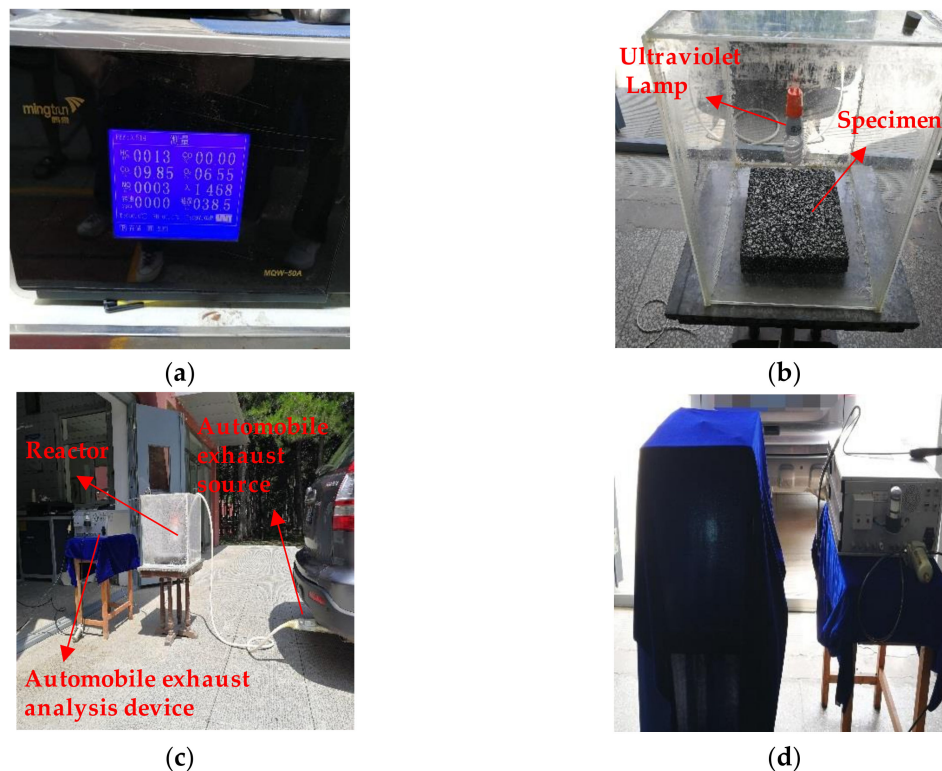


Figure 4. The apparatus of photocatalytic degradation experiment: (a) automobile exhaust analysis device; (b) reactor; (c) test device; (d) test process.

3.5. ESEM

The efficiency of photocatalytic automobile exhaust degradation is related to the contact area of nano TiO_2 and ultraviolet light. In this paper, the ESEM was adopted to obtain the microscopic characterization of nano TiO_2 . 17 points (shown in Figure 5a) on the surface of pervious concrete sample were selected as sampling points, and among them, 3 evenly selected measuring points were chosen for taking pictures. The samples were air-dried and gilded, and it should be noted that the observation surface of the concrete sample should not be damaged during the processing of the sample. The processed sample is shown in Figure 5b.

The processed sample was put into the ESEM observation room, the ESEM equipment is shown in Figure 6a, the sample on the worktable was leveled by silicon wafers or other dry materials to avoid errors caused during imaging. The picture taken by ESEM is shown in Figure 6b.

The Image-Pro Plus (Rockville, MD, USA) was used to process the picture and extract the area value of nano TiO_2 in the picture, and the area ratio of nano TiO_2 area to the measuring point area was

calculated and the average value of 51 measuring points were adopted to characterize the contact area of nano TiO₂ and ultraviolet light. The specific calculation is shown in Equation (3).

$$Area\ Ratio = \frac{\sum_{1}^{51} \frac{Area_T}{Area_{mp}}}{51} \quad (3)$$

where *Area Ratio* is the average value of 51 measuring points to characterize the ratio of nano TiO₂ area to the pervious concrete substrate materials; *Area_T* is the nano TiO₂ area of the measuring point; *Area_{mp}* is the area of measuring point.

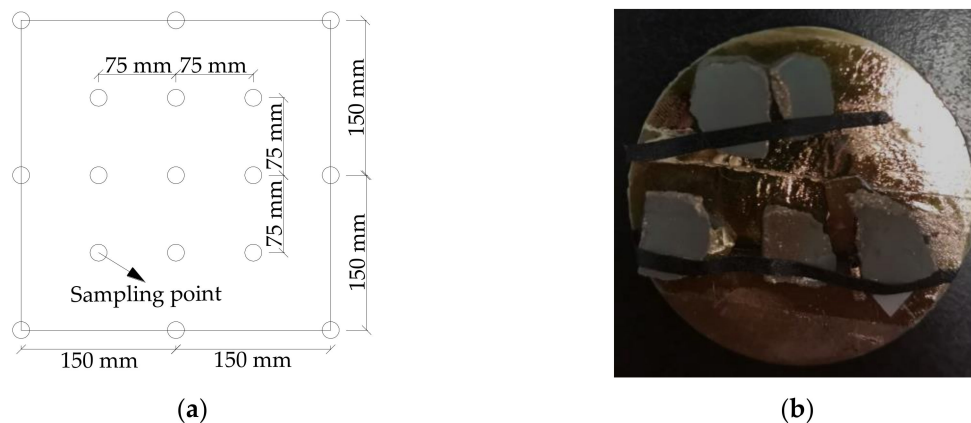


Figure 5. The sampling diagram and processed samples: (a) schematic diagram; (b) processed samples.

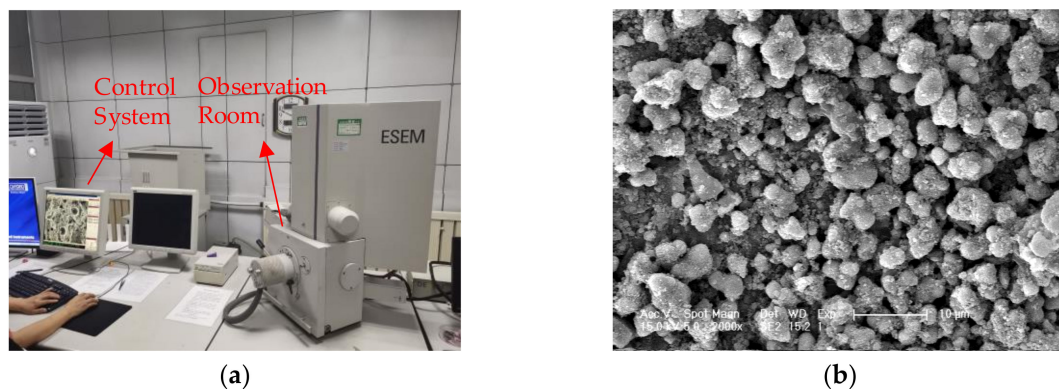


Figure 6. The environmental scanning electron microscope (ESEM) equipment and sample microscopic picture: (a) ESEM equipment; (b) sample microscopic picture.

4. Results

4.1. The Reaction Conditions for Photocatalytic Degradation

The experimental results of photocatalytic degradation of HC and NO_x by PEFPC and plain pervious concrete (PPC) with different light sources are shown in Figure 7. It can be seen from Figure 7 that the PPC cannot significantly photocatalytically degrade HC and NO_x, and only a small amount of HC and NO_x were consumed by PEFPC and PPC with dark conditions, while the PEFPC can significantly photocatalytically degrade HC and NO_x under the ultraviolet light irradiation condition. It can be concluded that photocatalyst and ultraviolet irradiation are the basic conditions for photocatalytic degradation of HC and NO_x. Figure 7 shows that the PEFPC can significantly photocatalytically degrade HC and NO_x under the sunlight irradiation condition. It indicates that

sunlight can stimulate the activity of nano TiO₂ on the surface of PEFPC and meet the basic requirements of photocatalytic reaction.

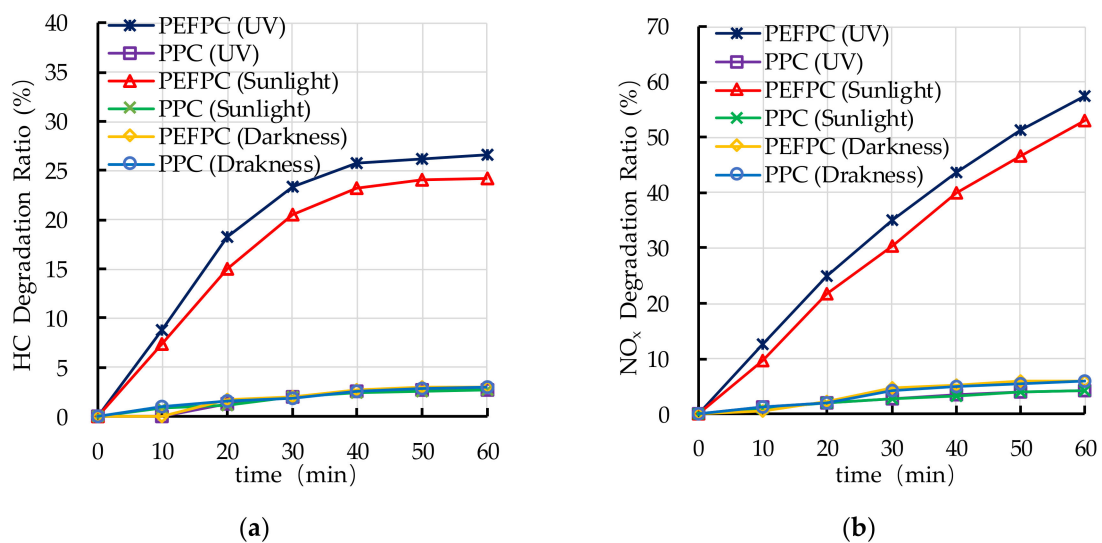


Figure 7. Effect of photocatalyst and light source on photocatalytic degradation of hydrocarbons (HC) and nitrogen oxides (NO_x): (a) HC degradation ratio; (b) NO_x degradation ratio.

4.2. Effect of Light Source on Photocatalytic Degradation

Ultraviolet irradiation is needed as an elementary condition for the photocatalytic degradation reaction. In this section, the effects of different light sources on photocatalytic degradation of automobile exhaust of PEFPC was studied. The selected light sources are ultraviolet height 135 mm, ultraviolet height 180 mm, ultraviolet height 225 mm, ultraviolet height 270 mm, sunlight, and darkness. The experimental results of photocatalytic degradation of HC are shown in Figure 8. It can be seen from Figure 8 that the photocatalytic degradation ratio of HC increases when the ultraviolet irradiation intensity increases from 31.8 $\mu\text{W}/\text{cm}^2$ to 105.1 $\mu\text{W}/\text{cm}^2$. The photocatalytic degradation ratio and rate of HC under ultraviolet light irradiation with a lamp height of 135 mm are similar to that under sunlight irradiation. The photocatalytic degradation ratios and rates of HC of ultraviolet height 180 mm, ultraviolet height 225 mm, and ultraviolet height 270 mm are lower than that of ultraviolet height 135 mm and sunlight.

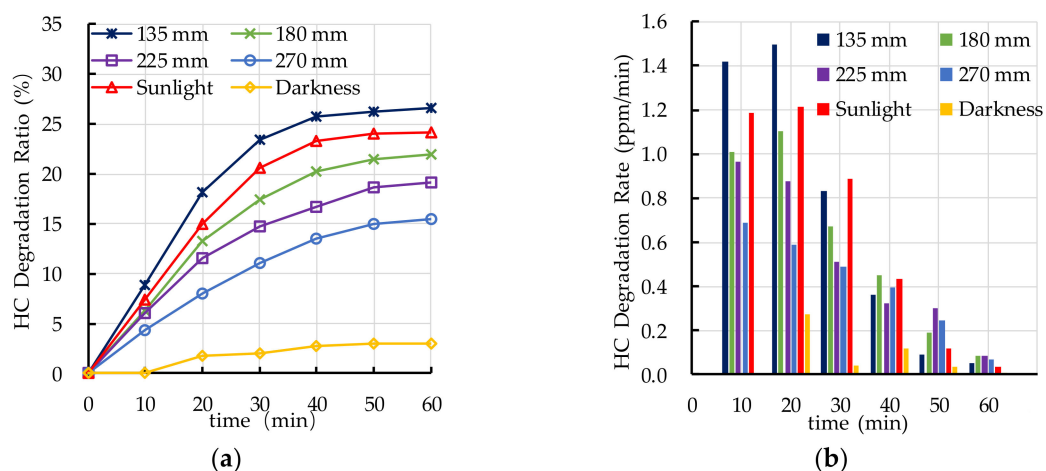


Figure 8. Effect of light source on photocatalytic degradation of HC: (a) HC degradation ratio; (b) HC degradation rate.

The experimental results of photocatalytic degradation of NO_x are shown in Figure 9. It can be seen that the photocatalytic degradation ratio of NO_x increases with the increasing in ultraviolet light irradiation intensity. The photocatalytic degradation ratio and rate of NO_x under ultraviolet light irradiation with a lamp height of 135 mm are similar to that under sunlight irradiation. The photocatalytic degradation ratios and rates of NO_x of ultraviolet lamp 180 mm, ultraviolet lamp 225 mm, and ultraviolet lamp 270 mm are lower than that of ultraviolet lamp 135 mm and sunlight. The experimental height of ultraviolet lamp in the following experiment is selected as 135 mm for the reason that the experimental results of photocatalytic degradation of HC and NO_x under ultraviolet light irradiation with a lamp height of 135 mm is similar to that under sunlight irradiation.

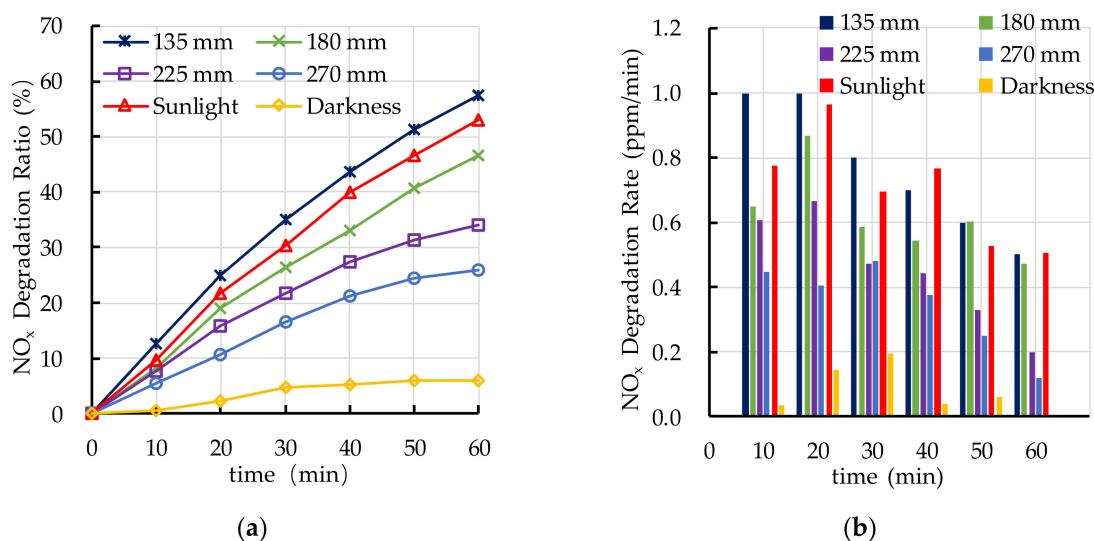


Figure 9. Effect of light source on photocatalytic degradation of NO_x : (a) NO_x degradation ratio; (b) NO_x degradation rate.

4.3. Effect of TiO_2 Particle Size on Photocatalytic Degradation

The experimental results of photocatalytic degradation of HC by PEFPC with different TiO_2 particle sizes are shown in Figure 10. The photocatalytic degradation ratio of 25 nm TiO_2 on degrading HC is better than that of 10 nm and 50 nm. The photocatalytic degradation rate of 25 nm TiO_2 is higher in the first 30 min and lower in the last 30 min than that of 10 nm and 50 nm, but overall, the photocatalytic degradation ratio of 25 nm is higher than that of 10 nm and 50 nm.

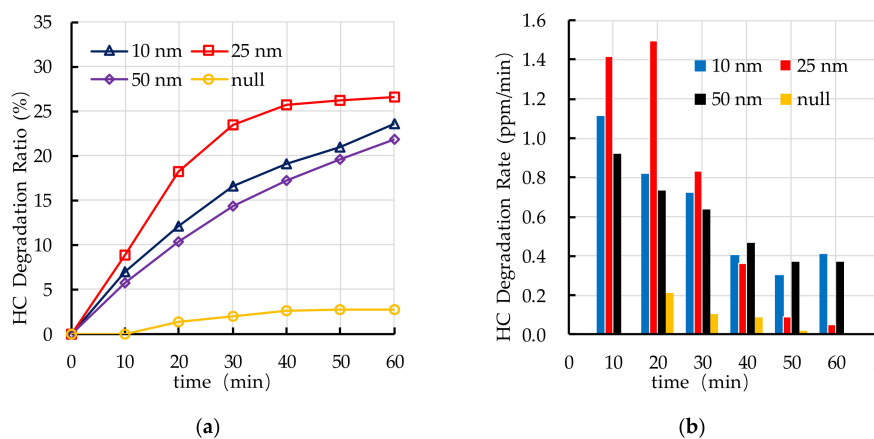


Figure 10. Effect of TiO_2 particle size on photocatalytic degradation of HC: (a) HC degradation ratio; (b) HC degradation rate.

Figure 11 shows the experimental results of photocatalytic degradation of NO_x by PEFPC with different TiO_2 particle sizes. The photocatalytic degradation ratio of 25 nm TiO_2 on degrading NO_x is the best, followed by 10 nm and 50 nm. The photocatalytic degradation ratio of PEFPC with three particle sizes reaches over 40% after 60 min. In addition, the average photocatalytic degradation rate of NO_x of 25 nm TiO_2 is 0.77 ppm/min, 10 nm TiO_2 is 0.64 ppm/min and 50 nm TiO_2 is 0.59 ppm/min.

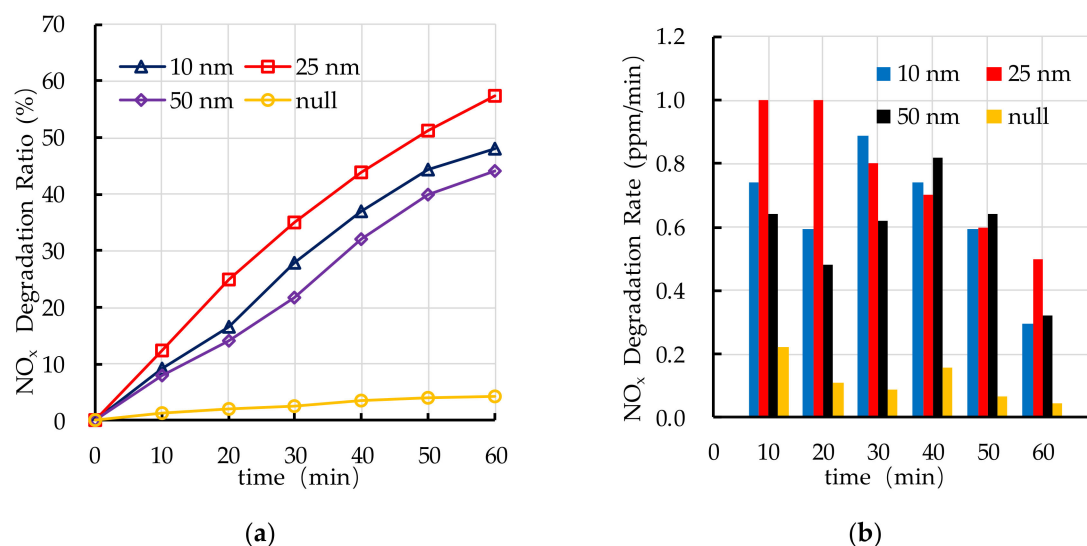


Figure 11. Effect of TiO_2 particle size on photocatalytic degradation of NO_x : (a) NO_x degradation ratio; (b) NO_x degradation rate.

4.4. Effect of TiO_2 Dosage on Photocatalytic Degradation

The effect of TiO_2 dosage on photocatalytic degradation of HC is shown in Figure 12. It is found that the TiO_2 dosage has a great impact on the photocatalytic degradation ratio of HC. When the TiO_2 dosage is larger than 10%, the photocatalytic degradation ratio of HC is better. The photocatalytic degradation ratio of HC increases with the increase of TiO_2 dosage (3–10%). When the TiO_2 dosage is 10–20%, the photocatalytic degradation ratio of HC changes little, which means that the 10% TiO_2 is enough and it can be used as the critical value for photocatalytic degradation of HC. When the TiO_2 dosage is 10%, the photocatalytic degradation rate of HC decreases with the increase of reaction time, it indicates that the reaction of photocatalytic degradation of HC mainly occurs in the first 30 min.

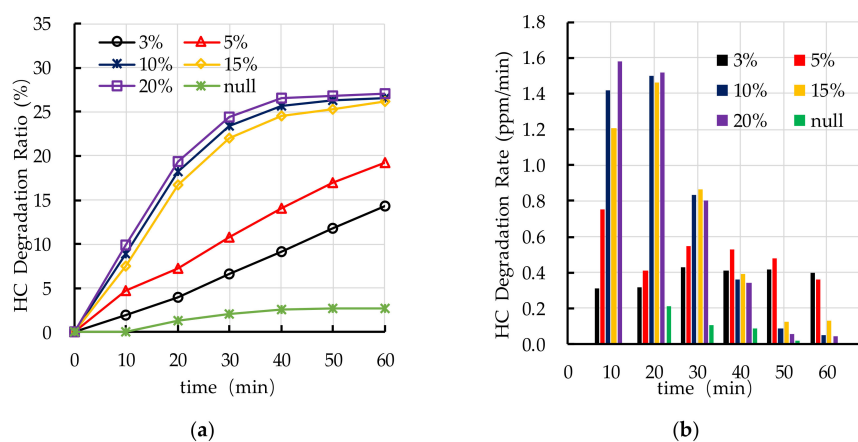


Figure 12. Effect of TiO_2 dosage on photocatalytic degradation of HC: (a) HC degradation ratio; (b) HC degradation rate.

Figure 13 shows the effect of TiO₂ dosage on photocatalytic degradation of NO_x. It can be seen that the photocatalytic degradation ratio of NO_x is the highest at 10% TiO₂ dosage and the photocatalytic degradation ratio reaches 59% at 60 min. When the TiO₂ dosage is 15% and 20%, the photocatalytic degradation ratio of NO_x is similar to that of 10%. The photocatalytic degradation rate of NO_x with different TiO₂ dosages is relatively stable. When the TiO₂ dosage is 10%, the average photocatalytic degradation rate of NO_x is highest, and the average rate is 0.77 ppm/min. It is observed that the photocatalytic degradation of automobile exhaust with 10% TiO₂ dosage is optimal.

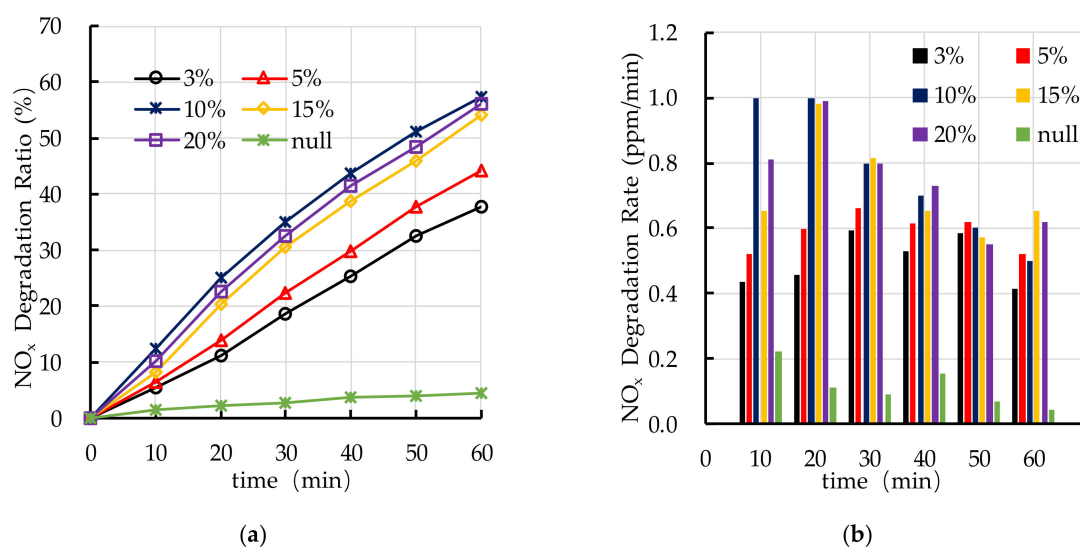


Figure 13. Effect of TiO₂ dosage on photocatalytic degradation of NO_x: (a) NO_x degradation ratio; (b) NO_x degradation rate.

4.5. Effect of TiO₂ Spraying Amount on Photocatalytic Degradation

Figure 14 shows the effects of different TiO₂ spraying amounts on photocatalytic degradation of HC. Figure 14a shows that the photocatalytic degradation ratio of HC of PEFPC with 30 g, 40 g, and 50 g TiO₂ spraying amounts is the best. Figure 14b shows that the photocatalytic degradation rate of HC in the first 30 min is higher than that in the last 30 min, it indicates that the photocatalytic activity of nano TiO₂ on the surface of PEFPC gradually decreases with the increase of reaction time. The reaction of photocatalytic degradation of HC mainly occurs in the first 30 min.

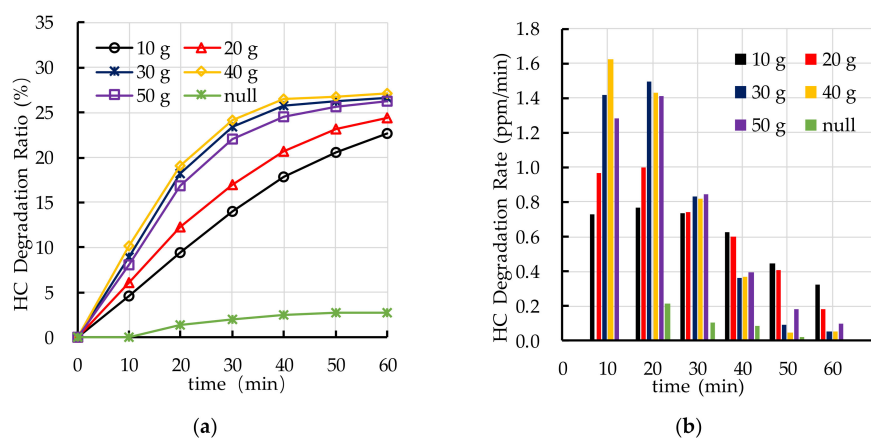


Figure 14. Effect of TiO₂ spraying amount on photocatalytic degradation of HC: (a) HC degradation ratio; (b) HC degradation rate.

Figure 15 shows the effects of different TiO₂ spraying amounts on photocatalytic degradation of NO_x. The results show that the photocatalytic degradation ratio of the specimen with 30 g TiO₂ spraying amount is the best. It is worth noting that the photocatalytic degradation ratio of NO_x of PEFPC increases with the increase of TiO₂ spraying amounts, when the TiO₂ spraying amounts is greater than 30 g, the photocatalytic degradation ratio of NO_x of PEFPC slightly decrease. In addition, comparing the reaction process of photocatalytic degradation of NO_x with that of HC, the photocatalytic degradation rate of NO_x is higher than that of HC, which means that photocatalytic degradation of NO_x by nano TiO₂ is more effective than that of HC. Based on the experimental results of photocatalytic degradation of HC and NO_x, the optimal TiO₂ spraying amount is 30 g (333.3 g/m²).

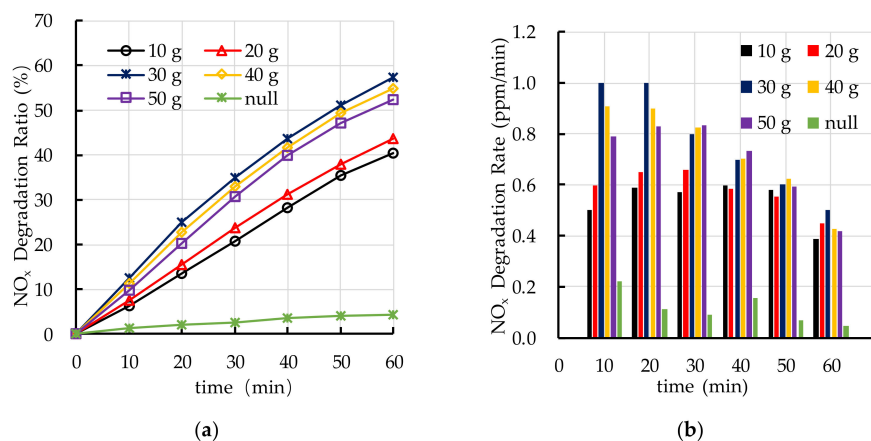


Figure 15. Effect of TiO₂ spraying amount on photocatalytic degradation of NO_x: (a) NO_x degradation ratio; (b) NO_x degradation rate.

4.6. Effect of Dispersant Dosage on Photocatalytic Degradation

Figure 16 shows the experimental results of photocatalytic degradation of HC by different dispersant dosages. The results show that dispersant has a positive effect on photocatalytic degradation of HC. However, excessive dispersant dosage (7.5–10.0%) has a negative effect on photocatalytic degradation of HC. Figure 16a shows that the photocatalytic degradation ratio of HC increases first and then decreases with the increase of dispersant dosage. Figure 16b shows that the photocatalytic degradation rate of HC gradually decreases with the increase of reaction time. The main stage of degradation of HC occurs in the first 30 min.

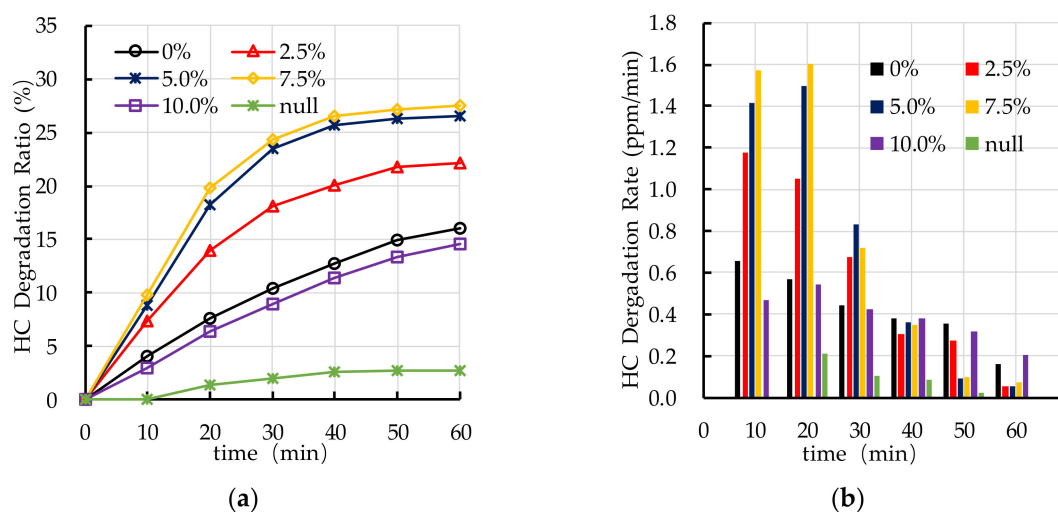


Figure 16. Effect of dispersant dosage on photocatalytic degradation of HC: (a) HC degradation ratio; (b) HC degradation rate.

Figure 17 shows the effects of different dispersant dosages on photocatalytic degradation of NO_x . The results show that dispersant has a great effect on photocatalytic degradation of NO_x . It can be observed that the photocatalytic degradation ratio of NO_x increases first with the increasing in dispersant dosage (0–5.0%) and then decreases with the increase of dispersant dosage (5.0–10.0%). The photocatalytic degradation rate of NO_x is relatively stable, which is different to the degradation of HC. Nano TiO_2 keeps good photocatalytic activity throughout the whole experiment. According to the experimental results of photocatalytic degradation of HC and NO_x , the optimal dispersant dosage is 5.0%.

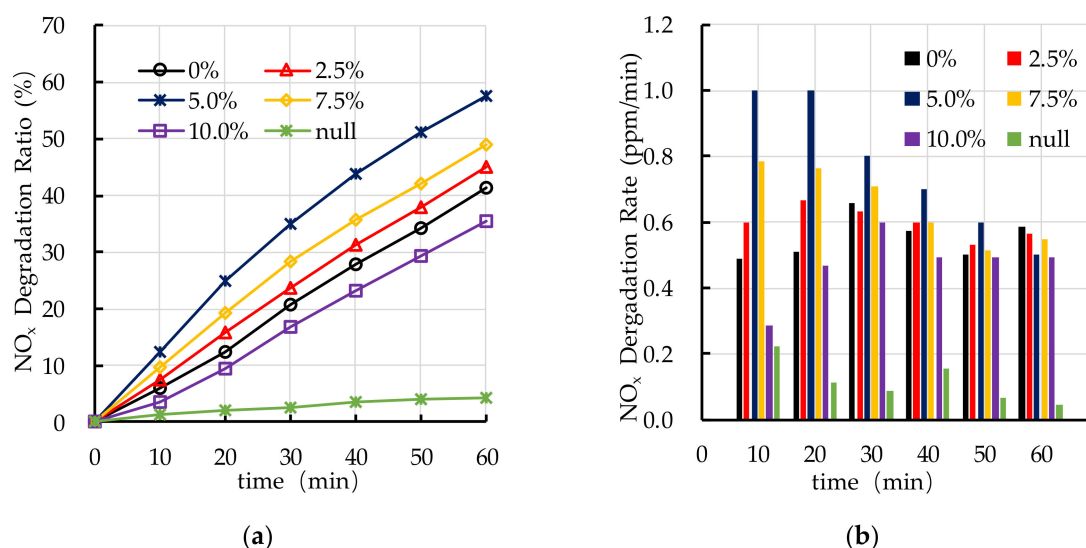


Figure 17. Effect of dispersant dosage on photocatalytic degradation of NO_x : (a) NO_x degradation ratio; (b) NO_x degradation rate.

5. Discussion

5.1. TiO_2 Particle Size

The experiment results of photocatalytic degradation reaction and the ESEM by different TiO_2 particle size are shown in Figure 18. When the photocatalytic degradation reaction is carried out for 60 min, the degradation ratio of HC and NO_x first increases and then decreases with the increasing in particle size, while the area ratio gradually decreases as the increasing in particle size. The increase in the area ratio means that the contact area of nano TiO_2 and ultraviolet light increases, which has a positive effect on the photocatalytic reaction. However, when the TiO_2 particle size is less than 25 nm, the degradation ratio of HC and NO_x increases as the area ratio decreases, which is related to the band gap of nano TiO_2 . When the particle size of nano TiO_2 is less than 10 nm, the band gap becomes larger, it indicates that the stronger photon energy is needed to activate electrons, which has a negative effect on the photocatalytic reaction [33].

5.2. TiO_2 Dosage

Figure 19 shows that the experiment results of photocatalytic degradation reaction and the ESEM by different TiO_2 dosage. The photocatalytic degradation ratio of HC and NO_x at 60 min increases as the nano TiO_2 dosage increases; while the nano TiO_2 dosage is 15%, the photocatalytic degradation ratio occurs slight decrease. However, overall, when the nano TiO_2 dosage is greater than 10%, the photocatalytic degradation ratio changes little. The area ratio has the same trend as the photocatalytic degradation ratio of HC and NO_x . It indicates that increasing the nano TiO_2 dosage has a positive effect on improving the contact area of nano TiO_2 and ultraviolet light. However, excessive nano TiO_2 particles, namely the nano TiO_2 dosage is greater than 10%, absorb and aggregate with each

other due to the VDW and coulomb force exist in the nano TiO_2 particles, which results the contact area change little. Therefore, it has little effect on the photocatalytic degradation of HC and NO_x .

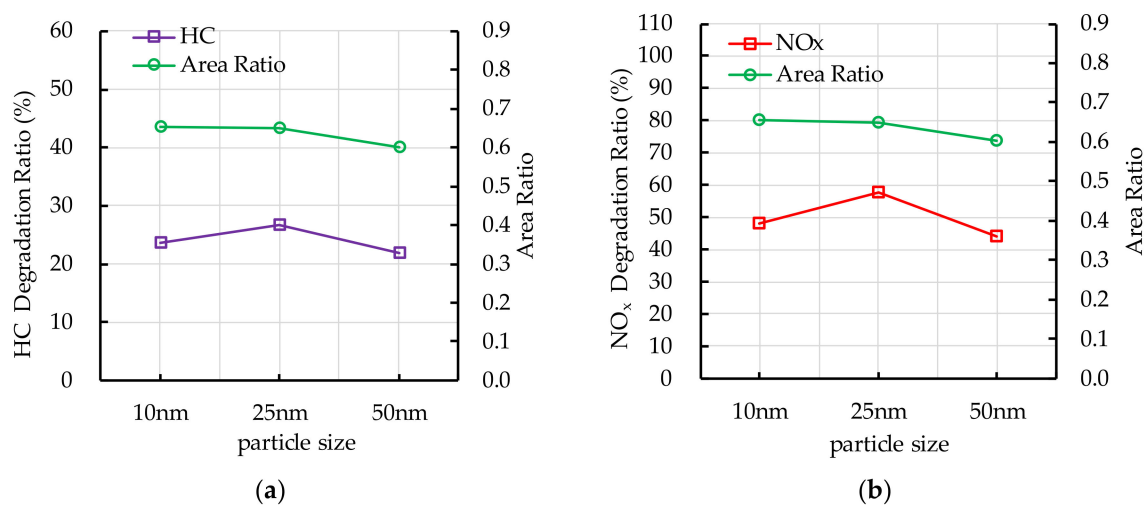


Figure 18. Effect of TiO_2 particle size on photocatalytic degradation and area ratio: (a) HC; (b) NO_x .

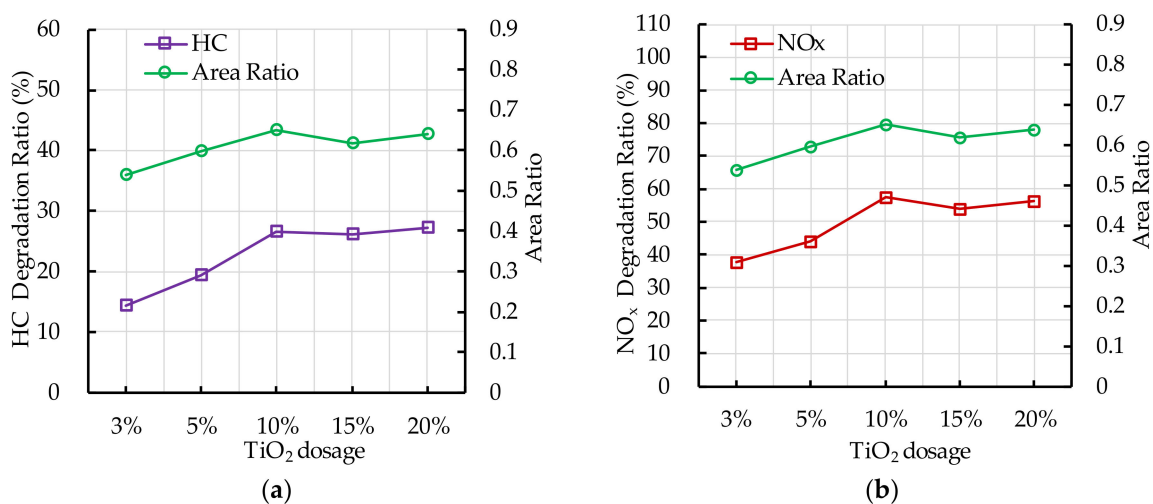


Figure 19. Effect of TiO_2 dosage on photocatalytic degradation and area ratio: (a) HC; (b) NO_x .

5.3. TiO_2 Spraying Amount

The experiment results of photocatalytic degradation reaction and the ESEM by different TiO_2 spraying amount are shown in Figure 20. The photocatalytic degradation ratios of HC and NO_x at the end of photocatalytic degradation reaction increase first and then decrease with the increase of nano TiO_2 spraying amount. The area ratio has the similar trend as the photocatalytic degradation ratio of HC and NO_x . It indicates that increasing the TiO_2 spraying amount has a positive effect on improving the contact area of nano TiO_2 and ultraviolet light. However, the excessive TiO_2 spraying amount, namely the TiO_2 spraying amount is greater than 30 g, leads to the nano TiO_2 particles absorbing and aggregating with each other and spraying film affects the nano TiO_2 particles absorb ultraviolet light, which results the contact area changes little or even slightly decreases. Therefore, it has slight negative effect on the photocatalytic degradation of HC and NO_x .

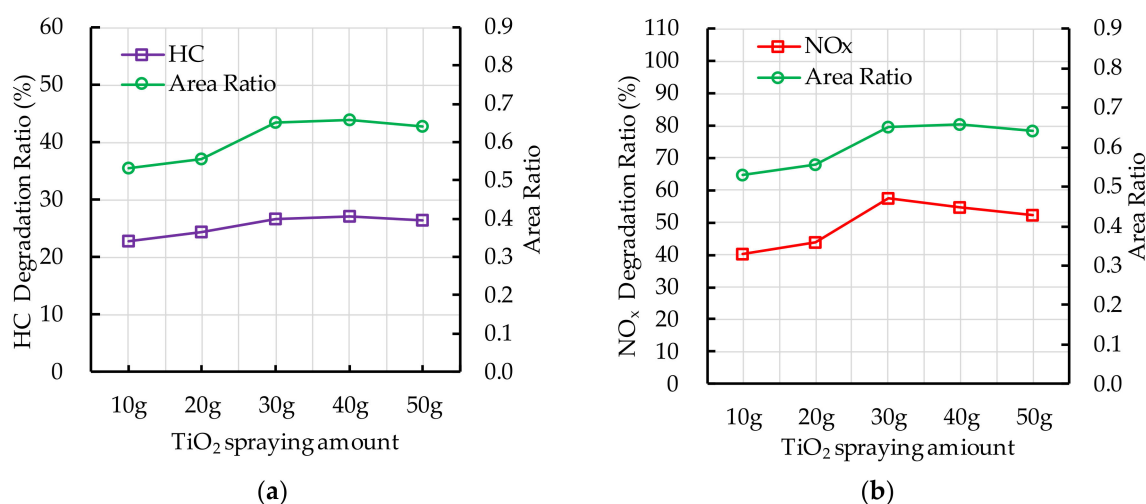


Figure 20. Effect of TiO₂ spraying amount on photocatalytic degradation and area ratio: (a) HC; (b) NO_x.

5.4. Dispersant Dosage

Figure 21 shows that the experiment results of photocatalytic degradation reaction and the ESEM by different dispersant dosage. When the photocatalytic degradation reaction lasts for 60 min, the photocatalytic degradation ratio of HC and NO_x first increases and then decreases with the increasing in dispersant dosage. The area ratio first increases and then decreases with the increasing in dispersant dosage. The change trend of area ratio is similar to the trend of photocatalytic degradation ratio of HC and NO_x. Adding dispersant has a positive effect on the dispersion stability of nano TiO₂ in the TiO₂ coating, therefore increasing the area ratio of TiO₂. However, excessive dispersant affects the dispersion stability of nano TiO₂. When the dispersant dosage reaches 10%, the dispersion stability of nano TiO₂ is worse than that of coating without dispersant, which has a negative effect on the photocatalytic degradation of HC and NO_x.

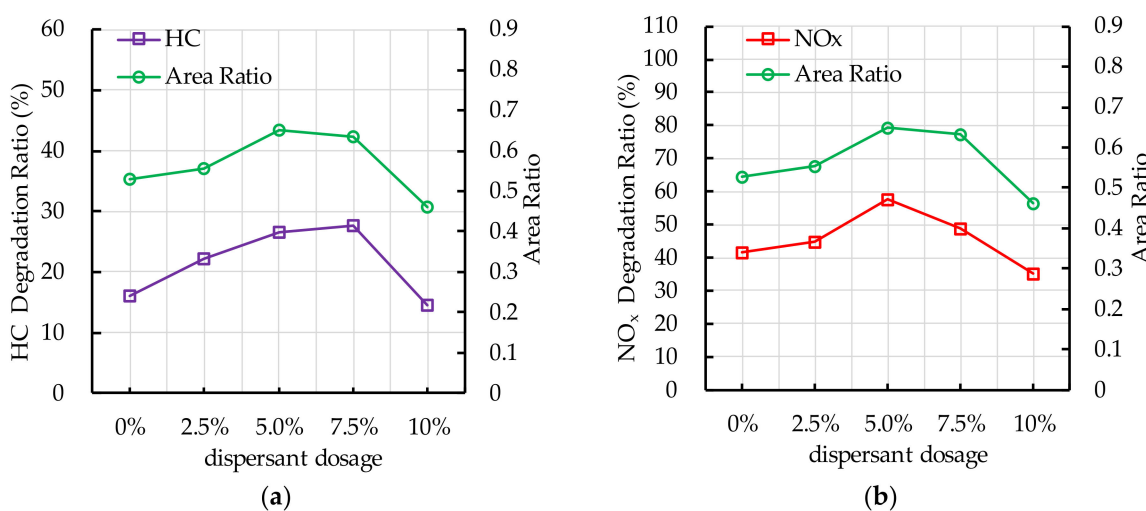


Figure 21. Effect of dispersant dosage on photocatalytic degradation and area ratio: (a) HC; (b) NO_x.

6. Conclusions

The photocatalytic performance of PEFFPC sprayed with TiO₂ was prepared and studied in the lab. The effects of light source, TiO₂ particle size, TiO₂ dosage, TiO₂ spraying amount, and dispersant dosage on the photocatalytic degradation were analyzed. Moreover, the distribution of nano TiO₂ was evaluated by the ESEM. Based on the results, the following conclusions can be drawn:

1. Ultraviolet irradiation is needed as an elementary condition for the photocatalytic degradation reaction. The photocatalytic degradation ratio of automobile exhaust increases with the increase of ultraviolet irradiation intensity. The PEFPC can effectively degrade automobile exhaust and significantly improve urban air quality.
2. The recommend nano TiO₂ particle size is 25 nm. The most ideal TiO₂ dosage and dispersant dosage are 10% and 5.0%, respectively. The optimal TiO₂ spraying amount is 333.3 g/m².
3. The photocatalytic degradation of HC and NO_x is different. The photocatalytic degradation of HC can be divided into two stages: rapid stage in the first 30 min and slow stage in the last 30 min. The photocatalytic degradation of NO_x is relatively stable.
4. The change in the photocatalytic ratio of PEFPC is consistent with the distribution area of nano TiO₂ on the surface of the substrate materials. The contact area between nano TiO₂ and ultraviolet light is a key factor affecting the photocatalytic performance of PEFPC.

Author Contributions: Conceptualization, G.L.; methodology, W.L., G.L. and X.L.; formal analysis, W.L. and X.L.; investigation, W.L. and X.L.; writing—original draft preparation, W.L.; writing—review and editing, G.L.; funding acquisition, H.L. All authors have read and agreed to the published version of the manuscript.

Funding: This research was funded by the Science Technology Development Program of Jilin Province (20180201026SF).

Acknowledgments: The authors would like to express their appreciation to the anonymous reviewers for their constructive suggestions and comments on improving the quality of the paper.

Conflicts of Interest: The authors declare no conflict of interest.

References

1. Shu, Y.J.; Ji, J.; Xu, Y.; Deng, J.G.; Huang, H.B.; He, M.; Leung, D.Y.C.; Wu, M.Y.; Liu, S.W.; Liu, S.L.; et al. Promotional role of Mn doping on catalytic oxidation of VOCs over mesoporous TiO₂ under vacuum ultraviolet (VUV) irradiation. *Appl. Catal. B Environ.* **2018**, *220*, 78–87. [[CrossRef](#)]
2. Huang, H.B.; Lu, H.X.; Zhan, Y.J.; Liu, G.Y.; Feng, Q.Y.; Huang, H.L.; Mu, M.Y.; Ye, X.G. VUV photo-oxidation of gaseous benzene combined with ozone-assisted catalytic oxidation: Effect on transition metal catalyst. *Appl. Surf. Sci.* **2017**, *391*, 662–667. [[CrossRef](#)]
3. Ângelo, J.; Andrade, L.; Madeira, L.M.; Mendes, A. An overview of photocatalysis phenomena applied to NO_x abatement. *J. Environ. Manag.* **2013**, *129*, 522–539. [[CrossRef](#)]
4. Čuček, L.; Klemeš, J.J.; Kravanja, Z. A Review of Footprint analysis tools for monitoring impacts on sustainability. *J. Clean. Prod.* **2019**, *34*, 9–20.
5. Shen, S.H.; Burton, M.; Jobson, B.; Haselbach, L. Pervious concrete with titanium dioxide as a photocatalyst compound for a greener urban road environment. *Constr. Build. Mater.* **2012**, *35*, 874–883. [[CrossRef](#)]
6. Nada, A.A.; Rouby, W.M.A.E.; Bekheet, M.F.; Antuch, M.; Weber, M.; Miele, P.; Viter, R.; Roualdes, S.; Millet, P.; Bechelany, M. Highly textured boron/nitrogen co-doped TiO₂ with honeycomb structure showing enhanced visible-light photoelectrocatalytic activity. *Appl. Surf. Sci.* **2020**, *505*, 144419. [[CrossRef](#)]
7. Nada, A.A.; Bekheet, M.F.; Viter, R.; Roualdes, S.; Bechelany, M. BN/Gd_xTi_(1-x)O_{(4-x)/2} nanofibers for enhanced photocatalytic hydrogen production under visible light. *Appl. Catal. B Environ.* **2019**, *251*, 76–86. [[CrossRef](#)]
8. Koca, M.; Kudas, Z.; Ekinici, D.; Aydoğan, S. Performance improvement of n-TiO₂/p-Si heterojunction by forming of n-TiO₂/polyphenylene/p-Si anisotype sandwich heterojunction. *Mat. Sci. ESEMicon. Proc.* **2021**, *121*, 105436. [[CrossRef](#)]
9. Bianchi, C.L.; Gatto, S.; Piroal, C.; Naldoni, A.; Michele, A.D.; Gerrato, G.; Crocellà, V.; Capucci, V. Photocatalytic degradation of acetone, acetaldehyde and toluene in gas-phase: Comparison between nano and micro-sized TiO₂. *Appl. Catal. B Environ.* **2014**, *146*, 123–130. [[CrossRef](#)]
10. Fu, P.F.; Zhang, P.Y.; Li, J. Photocatalytic degradation of low concentration formaldehyde and simultaneous elimination of ozone by-product using palladium modified TiO₂ films under UV 254+185nm irradiation. *Appl. Catal. B Environ.* **2011**, *105*, 220–228. [[CrossRef](#)]

11. Jo, W.K.; Kim, J.T. Application of visible-light photocatalysis with nitrogen-doped or unmodified titanium dioxide for control of indoor-level volatile organic compounds. *J. Hazard. Mater.* **2009**, *164*, 360–366. [[CrossRef](#)] [[PubMed](#)]
12. Guo, M.Z.; Poon, C.S. Photocatalytic NO removal of concrete surface layers intermixed with TiO₂. *Build. Environ.* **2013**, *70*, 102–109. [[CrossRef](#)]
13. Chen, J.; Poon, C.S. Photocatalytic activity of titanium dioxide modified concrete materials— Influence of utilizing recycled glass cullets as aggregates. *J. Environ. Manag.* **2009**, *90*, 3436–3442. [[CrossRef](#)] [[PubMed](#)]
14. Wang, H.M.; Xie, D.; Chen, Q.; You, C.F. Kinetic modeling for the deactivation of TiO₂ during the photocatalytic removal of low concentration SO₂. *Chem. Eng. J.* **2016**, *303*, 425–432. [[CrossRef](#)]
15. Shayegan, Z.; Lee, C.S.; Haghghat, F. TiO₂ photocatalyst for removal of volatile organic compounds in gas phase—A review. *Chem. Eng. J.* **2018**, *334*, 2408–2439. [[CrossRef](#)]
16. Yahia, A.; Kabagire, K.D. New approach to proportion pervious concrete. *Constr. Build. Mater.* **2014**, *62*, 38–46. [[CrossRef](#)]
17. Shen, W.G.; Zhang, C.; Li, Q.; Zhang, W.S.; Cao, L.; Ye, J.Y. Preparation of titanium dioxide nano particle modified photocatalytic self-cleaning concrete. *J. Clean. Prod.* **2015**, *87*, 762–765. [[CrossRef](#)]
18. Ballari, M.M.; Hunger, M.; Husken, G.; Brouwers, H.J.H. NO_x photocatalytic degradation employing concrete pavement containing titanium dioxide. *Appl. Catal. B Environ.* **2010**, *95*, 245–254. [[CrossRef](#)]
19. Ballari, M.M.; Yu, Q.L.; Brouwers, H.J.H. Experimental study of the NO and NO₂ degradation by photocatalytically active concrete. *Catal. Today* **2011**, *161*, 175–180. [[CrossRef](#)]
20. Henderson, M.A. A surface science perspective on TiO₂ photocatalysis. *Surf. Sci. Rep.* **2011**, *66*, 185–297. [[CrossRef](#)]
21. Guo, M.Z.; Ling, T.C.; Poon, C.S. Nano-TiO₂-based architectural mortar for NO removal and bacteria inactivation: Influence of coating and weathering conditions. *Cement Concrete Comp.* **2013**, *36*, 101–108. [[CrossRef](#)]
22. Nolam, N.T.; Seery, M.K.; Pillai, S.C. Spectroscopic Investigation of the Anatase-to-Rutile Transformation of Sol-Gel-Synthesized TiO₂ Photocatalysts. *J. Phys. Chem. C* **2009**, *113*, 16151–16157. [[CrossRef](#)]
23. Fischer, K.; Gawel, A.; Rosen, D.; Krause, M.; Latif, A.A.; Griebel, J.; Prager, A.; Schulze, A. Low-Temperature Synthesis of Anatase/Rutile/Brookite TiO₂ Nanoparticles on a Polymer Membrane for Photocatalysis. *Catalysts* **2017**, *7*, 209. [[CrossRef](#)]
24. Monai, M.; Montini, T.; Fornasiero, P. Brookite: Nothing New under the Sun ? *Catalysts* **2017**, *7*, 304. [[CrossRef](#)]
25. Xu, Y.D.; Chen, W.; Jin, R.Y.; Shen, J.S.; Smallbone, K.; Yan, C.Y.; Hu, L. Experimental investigation of photocatalytic effects of concrete in air purification adopting entire concrete waste reuse model. *J. Hazard. Mater.* **2018**, *353*, 421–430. [[CrossRef](#)]
26. Guo, M.Z.; Ling, T.C.; Poon, C.S. Photocatalytic NO_x degradation of concrete surface layers intermixed and spray-coated with nano-TiO₂: Influence of experimental factors. *Cement. Concr. Comp.* **2017**, *83*, 279–289. [[CrossRef](#)]
27. Dalton, J.S.; Janes, P.A.; Jones, N.G.; Nicholson, J.A.; Hallam, K.R.; Allen, G.C. Photocatalytic oxidation of NO_x gases using TiO₂: A surface spectroscopic approach. *Environ. Pollut.* **2002**, *120*, 415–422. [[CrossRef](#)]
28. Chen, J.; Poon, C.S. Photocatalytic construction and building materials: From fundamentals to applications. *Build. Environ.* **2009**, *44*, 1899–1906. [[CrossRef](#)]
29. Wu, Y.; Zhao, J.Z.; Li, Y.; Lu, K. Preparation and freezing behavior of TiO₂ nanoparticle suspensions. *Ceram. Int.* **2016**, *42*, 15597–15602. [[CrossRef](#)]
30. Ministry of Housing and Urban-Rural Development of the People’s Republic of China. *Technical Specifications for Pervious Concrete Pavement*; Ministry of Housing and Urban-Rural Development of the People’s Republic of China: Beijing, China, 2009. (In Chinese)
31. Liu, H.B.; Luo, G.B.; Wei, H.B.; Yu, H. Strength, permeability, and freeze-thaw durability of pervious concrete with different aggregate sizes, porosities, and water-binder ratios. *Appl. Sci.* **2018**, *8*, 1217. [[CrossRef](#)]

32. Liu, H.B.; Luo, G.B.; Gong, Y.F.; Wei, H.B. Mechanical properties, permeability, and freeze–thaw resistance of pervious concrete modified by waste crumb rubbers. *Appl. Sci.* **2018**, *8*, 1843. [[CrossRef](#)]
33. Kmat, P.V. Photochemistry on Nonreactive and Reactive (ESEMiconductor) Surfaces. *Chem. Rev.* **1993**, *93*, 267–300. [[CrossRef](#)]

Publisher’s Note: MDPI stays neutral with regard to jurisdictional claims in published maps and institutional affiliations.



© 2020 by the authors. Licensee MDPI, Basel, Switzerland. This article is an open access article distributed under the terms and conditions of the Creative Commons Attribution (CC BY) license (<http://creativecommons.org/licenses/by/4.0/>).